Fusion Engineering and Design 123 (2017) 607–611

Contents lists available at ScienceDirect

Fusion Engineering and Design

journal homepage: www.elsevier.com/locate/fusengdes

Nonlinear burn control using in-vessel coils and isotopic fueling in ITER

Andres Pajares*, Eugenio Schuster

Department of Mechanical Engineering and Mechanics, Lehigh University, Bethlehem, PA 18015, USA

HIGHLIGHTS

- Auxiliary power modulation has been traditionally employed for burn control.
- Fueling rate modulation can be used to directly control the plasma density.
- Moreover, fueling rate modulation can control the plasma energy by isotopic fueling.
- The in-vessel coil system is also a potential actuator to decrease the plasma energy.
- A nonlinear burn controller that integrates the three mentioned actuators is proposed in this work.

ARTICLE INFO

Article history:
Received 3 October 2016
Received in revised form 16 February 2017
Accepted 26 February 2017
Available online 31 March 2017

Keywords:
Nonlinear control
Burn control
Model-based control
Tokamak plasma control

ABSTRACT

In future burning tokamaks, active control of the plasma temperature and density will be necessary to produce a determined amount of fusion power. Conventional actuation methods, such as auxiliary power modulation and fueling rate modulation, are usually employed to tackle this so-called burn control problem. Fueling rate modulation can be used not only to directly control the plasma density but also to indirectly control the plasma energy by means of isotopic fuel tailoring. Moreover, based on recent experiments, the in-vessel coil system arises as a possible actuation method to decrease the plasma energy by generating non-axisymmetric fields in the plasma that may reduce the energy confinement time. In this work, a nonlinear burn controller that integrates the three mentioned actuators is proposed. The controller performance is tested via simulations for an ITER-like scenario.

1. Introduction

In ITER, steady-state operation with $Q \geq 10$ (Q is the ratio of fusion power to auxiliary power injected into the plasma) is expected [1]. In order to achieve such extended burning operation, control of the plasma temperature and density will be required to regulate the fusion power while avoiding potential thermal instabilities. This problem, known as burn control, requires the development of control algorithms that make use of the available actuators in the tokamak. Traditionally, modulation of the auxiliary power [2] (like neutral beam injection or radio-frequency heating) and modulation of the deuterium (D) and tritium (T) fueling rates [3] were actuators considered for burn control. Modulation of the fueling rates can be used to directly control the plasma density by regulating the D and T densities, denoted in this work as n_D and n_T, respectively. Moreover, modulation of the fueling rates can be used to indirectly control the plasma energy by modulating the tritium fraction γ, defined as $\gamma = n_T/(n_D + n_T)$. Such control approach, referred to as isotopic fuel tailoring, has been proven effective in previous work [4]. More recently, the in-vessel coil system has demonstrated its capability to control the plasma energy in DIII-D [5] by generating non-axisymmetric fields that modify the plasma energy confinement time, τ_E^*.

In this work, a model-based nonlinear burn controller is proposed. The use of nonlinear control techniques removes the limits imposed by linearization in previous work. The resulting controller can accommodate large perturbations and drive the system from one point to another during operation. The auxiliary power, the fueling rates (used to directly control the density or for isotopic fueling) and the in-vessel coil system are utilized as actuators. A zero-dimensional, nonlinear model is used to predict the time evolutions of the plasma energy and the densities of the different particles present in the plasma. Also, a model is proposed to characterize the influence of the in-vessel coil current on τ_E^*. The performance of the controller is tested via simulations for an ITER-like scenario.

* Corresponding author.
E-mail address: andres.pajares@lehigh.edu (A. Pajares).

http://dx.doi.org/10.1016/j.fusengdes.2017.02.098
0920-3796/

2. Burning plasma model

This model considers the presence of four different types of particles in the plasma: α-particles, D, T and impurities. The time evolution of the α-particle density, n_α, is given by

$$\frac{dn_\alpha}{dt} = -\frac{n_\alpha}{\tau_\alpha^*} + S_\alpha, \tag{1}$$

where τ_α^* is the α-particle confinement time and $S_\alpha = n_D n_T \langle\sigma v\rangle_{DT}$ is the source of α-particles produced by the fusion reaction, where $\langle\sigma v\rangle_{DT}$ is the D-T reactivity, which is a nonlinear function of the plasma temperature T [6]. The time evolutions of the D and T densities are given by

$$\frac{dn_D}{dt} = -\frac{n_D}{\tau_D} + f_{eff} S_D^R - S_\alpha + S_D^{inj}, \tag{2}$$

$$\frac{dn_T}{dt} = -\frac{n_T}{\tau_T} + f_{eff} S_T^R - S_\alpha + S_T^{inj}, \tag{3}$$

where τ_D and τ_T are the D and T particle confinement times, respectively, S_D^R and S_T^R are the sources of D and T particles from recycling, respectively, S_D^{inj} and S_T^{inj} are the controllable injection rates of D and T particles, respectively, and f_{eff} is a constant parameter that models the efficiency of the D and T particles recycling. The sources S_D^R and S_T^R are given by

$$S_D^R = \frac{1}{1 - f_{ref}(1 - f_{eff})} \times \left\{ f_{ref} \frac{n_D}{\tau_D} + (1 - \gamma_{PFC}) \left[\frac{(1 - f_{ref}(1 - f_{eff}))R_{eff}}{1 - R_{eff}(1 - f_{eff})} - f_{ref} \right] \left(\frac{n_D}{\tau_D} + \frac{n_T}{\tau_T} \right) \right\}, \tag{4}$$

$$S_T^R = \frac{1}{1 - f_{ref}(1 - f_{eff})} \times \left\{ f_{ref} \frac{n_T}{\tau_T} + \gamma_{PFC} \left[\frac{(1 - f_{ref}(1 - f_{eff}))R_{eff}}{1 - R_{eff}(1 - f_{eff})} - f_{ref} \right] \left(\frac{n_D}{\tau_D} + \frac{n_T}{\tau_T} \right) \right\}, \tag{5}$$

where f_{ref}, γ_{PFC} and R_{eff} are constant parameters that characterize the recycling effects [4].

The time evolution of the impurity particle density, n_I, is modeled as

$$\frac{dn_I}{dt} = -\frac{n_I}{\tau_I^*} + S_I^{sp}, \tag{6}$$

where τ_I^* is the impurity particle confinement time, and S_I^{sp} is the source of impurities arising from sputtering, which is modeled as

$$S_I^{sp} = f_I^{sp} \left(\frac{n}{\tau_I^*} + \frac{dn}{dt} \right), \tag{7}$$

where f_I^{sp} is a constant parameter that reflects the fact that there is always a content of impurities in the plasma, and n is the total plasma density, which is given by

$$n = n_i + n_e = n_\alpha + n_D + n_T + n_I + n_e, \tag{8}$$

where $n_i = n_\alpha + n_D + n_T + n_I$ is the ion density, and n_e is the electron density, which is related to the densities of the other particles by the quasi-neutrality condition

$$n_e = 2n_\alpha + n_D + n_T + Z_I n_I, \tag{9}$$

where Z_I is the atomic number of the impurities.

The plasma energy, E, balance is given by

$$\frac{dE}{dt} = -\frac{E}{\tau_E^*} + P_\alpha + P_{Ohm} - P_{rad} + P_{aux}, \tag{10}$$

where P_α is the heating power from α-particles, P_{Ohm} is the ohmic heating power, P_{rad} is the radiative power and P_{aux} is the auxiliary power injected by external controllable means. The α-particle power is given by $P_\alpha = Q_\alpha S_\alpha$, where Q_α = 3.52 MeV. The ohmic power is given by $P_{Ohm} = 2.8 \times 10^{-9} Z_{eff} I_p^2/(a^4 T^{3/2})$, where $Z_{eff} \triangleq (4n_\alpha + n_D + n_T + Z_I^2 n_I)/n_e$ is the effective atomic number of the plasma ions, I_p is the plasma current, a is the minor radius of the tokamak and T has to be given in keV. The radiative power is taken as $P_{rad} = P_{brem} + P_{line} + P_{rec}$, where P_{brem}, P_{line} and P_{rec} are the bremsstrahlung, line and recombination components, respectively, and each term is given by $P_{brem} = 4.8 \times 10^{-37} (\sum_i n_i Z_i^2) n_e \sqrt{T}$, $P_{line} = 1.8 \times 10^{-38} (\sum_i n_i Z_i^4) n_e T^{-1/2}$, and $P_{rec} = 4.1 \times 10^{-40} (\sum_i n_i Z_i^6) n_e T^{-3/2}$, where T has to be given in keV [7]. For τ_E^*, the IPB98(y,2) scaling [1] is used, i.e.

$$\tau_E^* = 0.0562 H_H^* I_p^{0.93} B_T^{0.15} n_{e19}^{0.41} M^{0.19} R^{1.97} \epsilon^{0.58} \kappa_{95}^{0.78} (PV)^{-0.69}, \tag{11}$$

where H_H^* is the so-called H-factor, I_p has to be given in MA, B_T is the toroidal magnetic field, n_{e19} is the electron density in $10^{19} m^{-3}$, $M = 3\gamma + 2(1-\gamma)$ is the effective mass of the plasma, R is major radius of the tokamak, $\epsilon = a/R$ is the aspect ratio, κ_{95} is the elongation at the 95% flux surface/separatrix, V is the plasma volume and $P = P_\alpha + P_{Ohm} - P_{rad} + P_{aux}$ is the total injected power, which has to be given in MW/m^3. It is assumed that all particle confinement times scale with τ_E^*, i.e., $\tau_\alpha^* = k_\alpha \tau_E^*$, $\tau_D = k_D \tau_E^*$, $\tau_T = k_T \tau_E^*$, $\tau_I = k_I \tau_E^*$, where k_α, k_D, k_T and k_I are constant parameters.

To simplify presentation, it is assumed that the electron temperature, T_e, and the ion temperature, T_i, are the same ($T_e = T_i = T$). The equation that relates E, n and T is

$$E = \frac{3}{2} nT. \tag{12}$$

The influence of the in-vessel coil current, I_{coil}, on τ_E^* is modeled through H_H^*. Based on the experimental data in [5] and the fact that higher collisionality and electron density discharges show smaller or null degradation in confinement when non-axisymmetric fields are applied [8,9], the following control-oriented model is proposed

$$H_H^* = H_H + \left(\frac{n_e}{n_{e,0}} \right)^{-\delta} \left(\frac{\nu_e^*}{\nu_{e,0}^*} \right)^{-\lambda} [C_2 I_{coil}^2 + C_1 I_{coil}], \tag{13}$$

where H_H is the value of the H-factor without operation of the in-vessel coil system, ν_e^* is the electron pedestal collisionality [8], and $\lambda > 0$, $\delta > 0$, $n_{e,0}$, $\nu_{e,0}^*$, C_1 and C_2 are constants that are determined from experimental data. Note that the in-vessel coils can only decrease τ_E^*, i.e., τ_E^* is maximum and $H_H^* = H_H$ when $I_{coil} = 0$, and $H_H^* < H_H$ for all $I_{coil} > 0$.

3. Control algorithm

The control objective is to drive the system to a particular working point characterized by the equilibrium of the dynamic equations (1), (2), (3), (6) and (10). By denoting $d()/dt \triangleq \dot{()}$, and writing the state variables as the sum of the equilibrium values, $\bar{x}$, plus a deviation, $\tilde{x}$, the dynamic equations (1), (2), (3), (6) and (10) become

$$\begin{aligned}
\dot{\tilde{n}}_\alpha &= -\frac{\bar{n}_\alpha}{\tau_\alpha^*} - \frac{\tilde{n}_\alpha}{\tau_\alpha^*} + S_\alpha, \quad \dot{\tilde{n}}_I = -\frac{\bar{n}_I}{\tau_I^*} - \frac{\tilde{n}_I}{\tau_I^*} + S_I^{sp}, \\
\dot{\tilde{n}}_D &= -\frac{\bar{n}_D}{\tau_D} - \frac{\tilde{n}_D}{\tau_D} + f_{eff} S_D^R - S_\alpha + S_D^{inj}, \\
\dot{\tilde{n}}_T &= -\frac{\bar{n}_T}{\tau_T} - \frac{\tilde{n}_T}{\tau_T} + f_{eff} S_T^R - S_\alpha + S_T^{inj}, \\
\dot{\tilde{E}} &= -\frac{\bar{E}}{\tau_E^*} - \frac{\tilde{E}}{\tau_E^*} + P_\alpha + P_{Ohm} - P_{rad} + P_{aux}.
\end{aligned} \tag{14}$$

The control objective is to drive the states in (14) to zero.

The first actuation method to control $\tilde{E}$ is the auxiliary power P_{aux}. The equation for $\tilde{E}$ in system (14) is reduced to

$$\dot{\tilde{E}} = -\left(\frac{1}{\tau_E^*} + K_E\right)\tilde{E} \tag{15}$$

just by setting

$$-\frac{\bar{E}}{\tau_E^*} + P_\alpha + P_{Ohm} - P_{rad} + P_{aux} = -K_E\tilde{E}, \tag{16}$$

where $K_E > 0$ is a design parameter. As $\tau_E^* > 0$, it is found that $\tilde{E} \to 0$ in time as long as condition (16) is fulfilled. Then, without saturation, the control law for P_{aux} is given by

$$P_{aux}^{unsat} = -K_E\tilde{E} - \frac{\bar{E}}{\tau_E^*} - P_\alpha - P_{Ohm} + P_{rad}. \tag{17}$$

When possible, the controller sets $P_{aux} = P_{aux}^{unsat}$, which assures that $\tilde{E} \to 0$. However, there exist saturation limits for P_{aux}, which are denoted as P_{aux}^{max} and P_{aux}^{min}. If $P_{aux}^{unsat} > P_{aux}^{max}$, the controller sets $P_{aux} = P_{aux}^{max}$, and then it cannot be assured that $\tilde{E} \to 0$. If after some time the energy subsystem is not stabilized, then it may be necessary to increase P_{aux}^{max}, or to improve τ_E^* by redesigning the machine parameters (I_p, B_T, etc.) in order to operate at this equilibrium point. If $P_{aux}^{unsat} < P_{aux}^{min}$, then the controller sets $P_{aux} = P_{aux}^{min}$, and the in-vessel coils are activated.

The second actuation method to control $\tilde{E}$ is the in-vessel coil system. The equation for $\tilde{E}$ in system (14) is reduced to

$$\dot{\tilde{E}} = -\left(\frac{1}{\tau_E^*} + K_{\tau_E}\right)\tilde{E}, \tag{18}$$

just by setting

$$-\frac{\bar{E}}{\tau_E^*} + P_\alpha + P_{Ohm} - P_{rad} + P_{aux}^{min} = -K_{\tau_E}\tilde{E}, \tag{19}$$

where $K_{\tau_E} > 0$ is a design parameter. As $\tau_E^* > 0$, it is found that $\tilde{E} \to 0$ as long as (19) is fulfilled, which can be achieved by setting τ_E^* to

$$(\tau_E^*)^{unsat} = \frac{\bar{E}}{P_\alpha + P_{Ohm} - P_{rad} + P_{aux}^{min} + K_{\tau_E}\tilde{E}}. \tag{20}$$

Then, (11), (13) and (20) allow for the computation of the unsaturated, stabilizing value of the in-vessel coil current, I_{coil}^{unsat}. Again, when possible, the controller sets $I_{coil} = I_{coil}^{unsat}$, which assures that $\tilde{E} \to 0$. Nonetheless, there exists a maximum current that can be driven in the in-vessel coil, that is denoted as I_{coil}^{max}. Note that the saturation case $I_{coil}^{unsat} < 0$ cannot be reached because the in-vessel coils only decrease τ_E^*. Then, if $I_{coil}^{unsat} > I_{coil}^{max}$, the controller sets $I_{coil} = I_{coil}^{max}$, but $\tilde{E} \to 0$ cannot be guaranteed. At that point, isotopic fueling is activated to regulate $\tilde{E}$.

The third actuation method to control $\tilde{E}$ is isotopic fueling. In this approach, control laws for S_D^{inj} and S_T^{inj} are sought to drive γ to a particular value, γ^*, such that the energy subsystem is stabilized. By taking into account that P_α can be rewritten as $P_\alpha = Q_\alpha\gamma(1-\gamma)(n_D+n_T)^2\langle\sigma v\rangle_{DT}$, γ^* is obtained from (16) as

$$\gamma^*(1-\gamma^*) = \frac{-K_E\tilde{E} - \bar{E}/\tau_E^*(I_{coil}^{max}) - P_{aux}^{min} - P_{Ohm} + P_{rad}}{Q_\alpha(n_D+n_T)^2\langle\sigma v\rangle_{DT}}, \tag{21}$$

where the least-tritium solution ($\gamma^* \le 0.5$) is taken. Note that $P_{aux} = P_{aux}^{min}$ and $I_{coil} = I_{coil}^{max}$ were assumed in (21). From (2), (3), and the definition of γ, it is possible to write

$$\dot{\gamma} = \gamma(1-\gamma)\left(\frac{1}{\tau_D} - \frac{1}{\tau_T}\right) + \frac{1}{n_D+n_T} \times \left\{f_{eff}S_T^R - S_\alpha + S_T^{inj} - \gamma\left[f_{eff}(S_D^R+S_T^R) - 2S_\alpha + S_D^{inj} + S_T^{inj}\right]\right\}. \tag{22}$$

By setting S_T^{inj} as

$$S_T^{inj,unsat} = \frac{\gamma[f_{eff}(S_D^R+S_T^R) - 2S_\alpha + S_D^{inj}]}{1-\gamma} + \frac{S_\alpha - f_{eff}S_T^R + \nu}{1-\gamma}, \tag{23}$$

Eq. (22) becomes

$$\dot{\gamma} = \gamma(1-\gamma)\left(\frac{1}{\tau_D} - \frac{1}{\tau_T}\right) + \frac{\nu}{n_D+n_T}, \tag{24}$$

and taking $\nu = -(n_D+n_T)[\gamma(1-\gamma)\frac{1}{\tau_D} + \gamma^2/\tau_T - u]$ makes

$$\dot{\gamma} = -\frac{\gamma}{\tau_T} + u. \tag{25}$$

By defining $\hat{\gamma} = \gamma - \gamma^*$, and neglecting $\dot{\gamma}^*$, (25) is rewritten as

$$\dot{\hat{\gamma}} = -\frac{\hat{\gamma}}{\tau_T} - \frac{\gamma^*}{\tau_T} + u. \tag{26}$$

By taking $u = \gamma^*/\tau_T - K_\gamma\hat{\gamma}$, where $K_\gamma > 0$ is a design parameter, (26) is reduced to $\dot{\hat{\gamma}} = -(1/\tau_T + K_\gamma)\hat{\gamma}$. Then, $\hat{\gamma} \to 0$ ($\gamma \to \gamma^*$). For S_D^{inj}, by taking

$$S_D^{inj,unsat} = -f_{eff}S_D^R + S_\alpha + \frac{\bar{n}_D}{\tau_D} - K_D\tilde{n}_D, \tag{27}$$

the $\tilde{n}_D$ Eq. in (14) is reduced to $\dot{\tilde{n}}_D = -(1/\tau_D + K_D)\tilde{n}_D$, which assures $\tilde{n}_D \to 0$. As $\gamma \to \gamma^*$ and $n_D \to \bar{n}_D$, then $n_T \to \bar{n}_D\gamma^*/(1-\gamma^*) \doteq n_T^*$, which is not $\bar{n}_T$, but is a bounded value. Then, when the controller attempts to control $\tilde{E}$ by means of isotopic fueling, it is expectable that neither n nor P_α go to their equilibrium values, but will be bounded. When possible, the controller sets $S_D^{inj} = S_D^{inj,unsat}$ and $S_T^{inj} = S_T^{inj,unsat}$ as in (27) and (23). However, it may happen that the fuel injectors saturate to their maximum or minimum values, that are denoted as $S_{D/T}^{inj,max}$ and $S_{D/T}^{inj,min}$, and then it cannot be assured that $\tilde{E} \to 0$. The density could increase to unacceptable limits, like the Greenwald electron density limit (defined as $n_G = I_p/(\pi a^2) \times 10^{14}\,m^{-3}$), in which disruptions that terminate the confined plasma take place. To prevent such situation, it is chosen that the controller attempts to regulate $\tilde{E}$ with the saturated values of S_D^{inj} and S_T^{inj} only if $n_e \le f_n n_G$, where $f_n \le 1$. If such condition is violated, then $\tilde{E}$ is not regulated and the next step is used instead.

In this fourth step, n and γ are directly controlled by means of fueling rate modulation. The fueling injectors are always used in this mode except if, as indicated in previous steps, isotopic fueling is required under acceptable density limits. Using (8) and (9), it is possible to write $\tilde{n} = n - \bar{n} = 3\tilde{n}_\alpha + 2(\tilde{n}_D + \tilde{n}_T) + (1+Z_I)\tilde{n}_I$. If S_T^{inj} is chosen as in (23) with $\nu = -(n_D+n_T)[\gamma(1-\gamma)(1/\tau_D) + \gamma^2/\tau_T - \bar{\gamma}/\tau_T - K_\gamma(\gamma-\bar{\gamma})]$, and S_D^{inj} is taken as

$$S_D^{inj,unsat} = \frac{n_D}{\tau_D} + \frac{n_D}{\tau_T} - f_{eff}(S_D^R + S_T^R) + 2S_\alpha - S_T^{inj,unsat} + w, \tag{28}$$

where $w = -1/2[3\tilde{n}_\alpha + (1+Z_I)\tilde{n}_I + K_D\tilde{n}]$, it is found that $\dot{\tilde{n}} = -K_D\tilde{n}$ and $\dot{\gamma} = -K_\gamma(\gamma - \bar{\gamma})$. Then, it can be assured that $\tilde{n} \to 0$, $\gamma \to \bar{\gamma}$. The controller sets $S_D^{inj} = S_D^{inj,unsat}$ and $S_T^{inj} = S_T^{inj,unsat}$ as in (28) and (23) when possible, and in case of saturation, the minimum or maximum values are set. Barring situations in which the fueling injectors are saturated for too long periods of time, it can be assured that $\tilde{n} \to 0$ and $\gamma \to \bar{\gamma}$.

Finally, it is shown that $n_\alpha \to \bar{n}_\alpha$ and $n_I \to \bar{n}_I$, provided that $n \to \bar{n}$, $\gamma \to \bar{\gamma}$ and $E \to \bar{E}$. By defining $\hat{n}_I = n_I - f_I^{sp}n$, (6) can be rewritten as $\dot{\hat{n}}_I + f_I^{sp}\dot{n} = -(\hat{n}_I + f_I^{sp}n)/\tau_I^* + S_I^{sp}$, and using (7), it is found that $\dot{\hat{n}}_I = -\hat{n}_I/\tau_I^*$, i.e., $\hat{n}_I \to 0$ ($\tau_I^* > 0$). Then, $n_I \to f_I^{sp}n = \bar{n}_I$. By focusing on (1), it can be noted that positive perturbations in n_α ($\tilde{n}_\alpha > 0$) decrease the first term $-n_\alpha/\tau_\alpha^*$. For the second term S_α, it can be noted that as $\gamma \to \bar{\gamma}$ and $T = \bar{E}/(\frac{3}{2}\bar{n}) \to \bar{T}$ from (12), then $S_\alpha \to \bar{\gamma}(1-\bar{\gamma})(n_D+n_T)^2\langle\bar{\sigma v}\rangle_{DT}$. Using $n \to \bar{n}$ and $n_I \to \bar{n}_I$, (8)

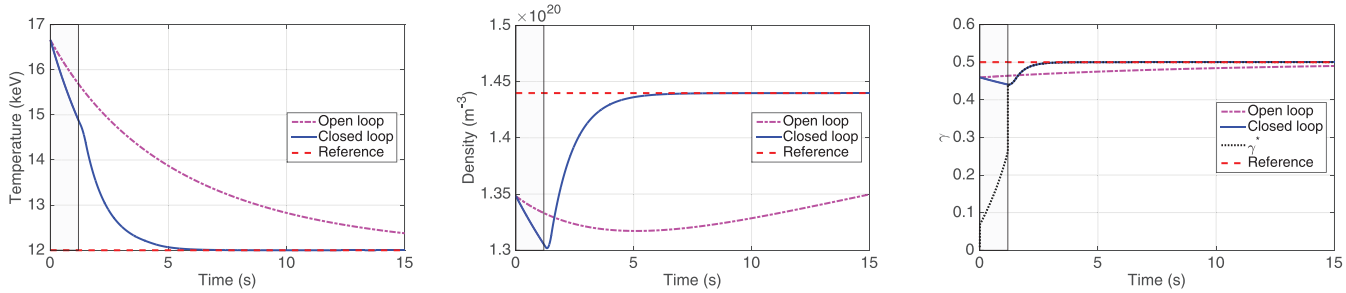

Fig. 1. Time evolution for the plasma temperature T, total plasma density n, and tritium fractions γ and γ^*. Isotopic fueling is used in the shaded region.

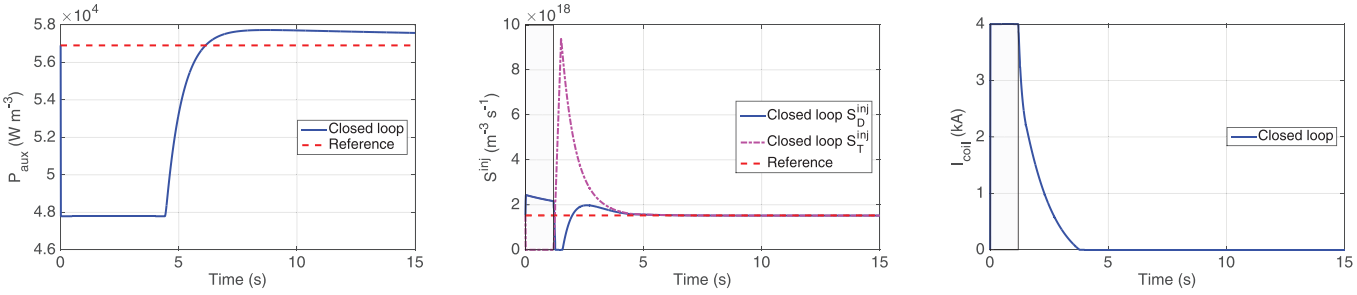

Fig. 2. Time evolution for the auxiliary power P_{aux}, fuel injection rates S_D^{inj} and S_T^{inj}, and in-vessel coil current I_{coil}. Isotopic fueling is used in the shaded region.

and (9) yield $(n_D + n_T) \to \frac{1}{2}[\bar{n} - 3(\tilde{n}_\alpha + \tilde{n}_\alpha) - (1 + Z_I)\tilde{n}_I]$. It can be noted that $\tilde{n}_\alpha > 0$ implies a decrease in $n_D + n_T$, so S_α decreases too. On the other hand, for negative perturbations in n_α ($\tilde{n}_\alpha < 0$), $n_D + n_T$ increases and S_α increases. This allows to write Eq. (1) as $\dot{\tilde{n}}_\alpha = -\phi_\alpha \tilde{n}_\alpha$, where ϕ_α is some positive function. As $\phi_\alpha > 0$, the α-particle density subsystem is exponentially stable. Therefore, it can be concluded that $\tilde{n}_\alpha \to 0$ and $n_\alpha \to \bar{n}_\alpha$.

4. Simulation results

The controller performance is tested by simulation for an ITER-like scenario [1]. The machine parameters are $I_p = 15$ MA, $B_T = 5.3$ T, $R = 6.2$ m, $a = 2$ m, $\kappa_{95} = 1.7$ and $V = 837$ m^3. The recycling parameters are taken as $f_{eff} = 0.2$, $f_{ref} = 0.7$, $\gamma_{PFC} = 0.4$ and $R_{eff} = 0.9$, which represent feasible values of these parameters [4]. The confinement parameters are taken as $H_H = 1.15$, $k_\alpha = 5$, $k_D = k_T = 2.5$ and, for simplicity, the only impurity considered is Beryllium ($Z_I = 4$) with $k_I = 10$ and $f_I = 0.02$. The actuation limits are taken as $P_{aux}^{max} = 73/V$ MW m^{-3}, $P_{aux}^{min} = 40/V$ MW m^{-3}, $S_{D/T}^{inj,min} = 0$, $S_{D/T}^{inj,max} = 3\times10^{19}$ m^{-3} s^{-1}, $\dot{S}_{D/T}^{max} = 3\times10^{19}$ m^{-3} s^{-2}, and $I_{coil}^{max} = 4$ kA. To estimate the constants in (13), it is assumed that the plasma in ITER will present a similar behavior as in DIII-D, and so experimental data in [5,9] is used. It is found that $C_1 = 0.0158$, $C_2 = -0.1524$, $n_{e,0} = 3.5\times10^{19}$ m^{-3} $\nu^*_{e,0} = 0.11$, $\lambda = 1$ and $\delta = 1$. Also, based on [5], it is assumed that the plasma shape, and then a, κ_{95} and V, do not change significantly under operation of the in-vessel coil system.

In this simulation study, the controller attempts to drive the system from a perturbed initial condition (-15% in n_D and +30% in E, which could simulate a temporary failure in the D fueling line with a thermal excursion) to a working point defined by $\bar{n} = 1.44 \times 10^{20}$, $\bar{T} = 12$ keV and $\bar{\gamma} = 0.5$. For simplicity, a constant value $\nu^*_e = \nu^*_{e,0}$ is taken, as ν^*_e in ITER will be small [8]. Also, $f_n = 0.9$ is taken. Fig. 1 shows the evolution for n, T and γ in open-loop and closed-loop simulations. Fig. 2 shows the evolution for the inputs S_D^{inj}, S_D^{inj}, P_{aux} and I_{coil}. It can be seen that the disturbance in the initial conditions is rejected in closed loop and the system is driven to the equilibrium within approximately 7 s, while the system evolution is considerably slower in open loop. At the beginning, P_{aux} and I_{coil} saturate due to the large $\tilde{E}$, so the controller uses the fuel injectors in isotopic fueling mode (shaded region). In such region, it can be seen that $\gamma \to \gamma^*$, and also that n drifts as it is not driven to $\bar{n}$. Once $\tilde{E}$ has been reduced and desaturation of I_{coil} is allowed, the fuel injectors are used to directly control n and γ, while I_{coil} and P_{aux} are used to regulate $\tilde{E}$. It can be noted P_{aux} does not reach its equilibrium value within the simulation time shown. The evolution of n triggers an increase in n_I, which produces significant P_{rad} that needs to be compensated by P_{aux}.

5. Summary and future work

In this work, a nonlinear controller has been presented which is capable of rejecting large initial perturbations and driving the system to a desired operating point by making use of the available actuators in a quite efficient way. This is the first burn controller to combine the traditional actuators, like auxiliary power and fueling rate modulation, with energy-control fueling-techniques, like isotopic fueling, and a proposed, novel actuator like the in-vessel coil system. Future work may include the development of robust versions of this controller as well as experimental testing by burn condition emulation.

Acknowledgements

Work supported by the US DoE (DE-SC0010661).

References

[1] Summary of the ITER final design report, Technical Report, International Atomic Energy Agency, 2001.
[2] E.A. Chaniotakis, J.P. Freidberg, D.R. Cohn, CIT burn control using auxiliary power modulation, Proceedings of the 13th IEEE Symposium on Fusion Engineering 1 (1989) 400–403.
[3] W. Hui, et al., Robust burn control of a fusion reactor by modulation of the refueling rate, Fusion Technol. 25 (3) (1994) 318–325.
[4] M.D. Boyer, E. Schuster, Nonlinear burn condition control in tokamaks using isotopic fuel tailoring, Nucl. Fusion 55 (8) (2015).

[5] R.J. Hawryluk, et al., Control of plasma stored energy for burn control using DIII-D in-vessel coils, Nucl. Fusion 55 (5) (2015).
[6] L.M. Hively, Convenient computational forms for Maxwellian reactivities, Nucl. Fusion 17 (4) (1977) 873.
[7] W.M. Stacey, Fusion: An Introduction to the Physics and Technology of Magnetic Confinement Fusion, 2nd ed., Wiley-VHC, Weinheim, 2010.
[8] T.E. Evans, et al., Edge stability and transport control with resonant magnetic perturbations in collisionless tokamak plasmas, Nat. Phys. 2 (2006) 419–423.
[9] T.E. Evans, et al., Suppression and mitigation of Edge-Localized Modes in the DIII-D tokamak with 3D magnetic perturbations, Plasma Fusion Res. 7 (2012).